BABAR Analysis Document #622, Version 2
BABAR-PUB-03/00
SLAC-PUB-0000
hep-ex/0000000

Measurements of the Branching Fractions of Charged B Decays to $K^{\pm}\pi^{\mp}\pi^{\pm}$ Final States

B. Aubert,[1] R. Barate,[1] D. Boutigny,[1] J.-M. Gaillard,[1] A. Hicheur,[1] Y. Karyotakis,[1] J. P. Lees,[1] P. Robbe,[1] V. Tisserand,[1] A. Zghiche,[1] A. Palano,[2] A. Pompili,[2] J. C. Chen,[3] N. D. Qi,[3] G. Rong,[3] P. Wang,[3] Y. S. Zhu,[3] G. Eigen,[4] I. Ofte,[4] B. Stugu,[4] G. S. Abrams,[5] A. W. Borgland,[5] A. B. Breon,[5] D. N. Brown,[5] J. Button-Shafer,[5] R. N. Cahn,[5] E. Charles,[5] C. T. Day,[5] M. S. Gill,[5] A. V. Gritsan,[5] Y. Groysman,[5] R. G. Jacobsen,[5] R. W. Kadel,[5] J. Kadyk,[5] L. T. Kerth,[5] Yu. G. Kolomensky,[5] J. F. Kral,[5] G. Kukartsev,[5] C. LeClerc,[5] M. E. Levi,[5] G. Lynch,[5] L. M. Mir,[5] P. J. Oddone,[5] T. J. Orimoto,[5] M. Pripstein,[5] N. A. Roe,[5] A. Romosan,[5] M. T. Ronan,[5] V. G. Shelkov,[5] A. V. Telnov,[5] W. A. Wenzel,[5] K. Ford,[6] T. J. Harrison,[6] C. M. Hawkes,[6] D. J. Knowles,[6] S. E. Morgan,[6] R. C. Penny,[6] A. T. Watson,[6] N. K. Watson,[6] T. Deppermann,[7] K. Goetzen,[7] H. Koch,[7] B. Lewandowski,[7] M. Pelizaeus,[7] K. Peters,[7] H. Schmuecker,[7] M. Steinke,[7] N. R. Barlow,[8] J. T. Boyd,[8] N. Chevalier,[8] W. N. Cottingham,[8] M. P. Kelly,[8] T. E. Latham,[8] C. Mackay,[8] F. F. Wilson,[8] K. Abe,[9] T. Cuhadar-Donszelmann,[9] C. Hearty,[9] T. S. Mattison,[9] J. A. McKenna,[9] D. Thiessen,[9] P. Kyberd,[10] A. K. McKemey,[10] V. E. Blinov,[11] A. D. Bukin,[11] V. B. Golubev,[11] V. N. Ivanchenko,[11] E. A. Kravchenko,[11] A. P. Onuchin,[11] S. I. Serednyakov,[11] Yu. I. Skovpen,[11] E. P. Solodov,[11] A. N. Yushkov,[11] D. Best,[12] M. Chao,[12] D. Kirkby,[12] A. J. Lankford,[12] M. Mandelkern,[12] S. McMahon,[12] R. K. Mommsen,[12] W. Roethel,[12] D. P. Stoker,[12] C. Buchanan,[13] D. del Re,[14] H. K. Hadavand,[14] E. J. Hill,[14] D. B. MacFarlane,[14] H. P. Paar,[14] Sh. Rahatlou,[14] U. Schwanke,[14] V. Sharma,[14] J. W. Berryhill,[15] C. Campagnari,[15] B. Dahmes,[15] N. Kuznetsova,[15] S. L. Levy,[15] O. Long,[15] A. Lu,[15] M. A. Mazur,[15] J. D. Richman,[15] W. Verkerke,[15] T. W. Beck,[16] J. Beringer,[16] A. M. Eisner,[16] C. A. Heusch,[16] W. S. Lockman,[16] T. Schalk,[16] R. E. Schmitz,[16] B. A. Schumm,[16] A. Seiden,[16] M. Turri,[16] W. Walkowiak,[16] D. C. Williams,[16] M. G. Wilson,[16] J. Albert,[17] E. Chen,[17] G. P. Dubois-Felsmann,[17] A. Dvoretskii,[17] D. G. Hitlin,[17] I. Narsky,[17] F. C. Porter,[17] A. Ryd,[17] A. Samuel,[17] S. Yang,[17] S. Jayatilleke,[18] G. Mancinelli,[18] B. T. Meadows,[18] M. D. Sokoloff,[18] T. Abe,[19] T. Barillari,[19] F. Blanc,[19] P. Bloom,[19] P. J. Clark,[19] W. T. Ford,[19] U. Nauenberg,[19] A. Olivas,[19] P. Rankin,[19] J. Roy,[19] J. G. Smith,[19] W. C. van Hoek,[19] L. Zhang,[19] J. L. Harton,[20] T. Hu,[20] A. Soffer,[20] W. H. Toki,[20] R. J. Wilson,[20] J. Zhang,[20] D. Altenburg,[21] T. Brandt,[21] J. Brose,[21] T. Colberg,[21] M. Dickopp,[21] R. S. Dubitzky,[21] A. Hauke,[21] H. M. Lacker,[21] E. Maly,[21] R. Müller-Pfefferkorn,[21] R. Nogowski,[21] S. Otto,[21] K. R. Schubert,[21] R. Schwierz,[21] B. Spaan,[21] L. Wilden,[21] D. Bernard,[22] G. R. Bonneaud,[22] F. Brochard,[22] J. Cohen-Tanugi,[22] Ch. Thiebaux,[22] G. Vasileiadis,[22] M. Verderi,[22] A. Khan,[23] D. Lavin,[23] F. Muheim,[23] S. Playfer,[23] J. E. Swain,[23] J. Tinslay,[23] M. Andreotti,[24] D. Bettoni,[24] C. Bozzi,[24] R. Calabrese,[24] G. Cibinetto,[24] E. Luppi,[24] M. Negrini,[24] L. Piemontese,[24] A. Sarti,[24] E. Treadwell,[25] F. Anulli,[26,*] R. Baldini-Ferroli,[26] A. Calcaterra,[26] R. de Sangro,[26] D. Falciai,[26] G. Finocchiaro,[26] P. Patteri,[26] I. M. Peruzzi,[26,*] M. Piccolo,[26] A. Zallo,[26] A. Buzzo,[27] R. Contri,[27] G. Crosetti,[27] M. Lo Vetere,[27] M. Macri,[27] M. R. Monge,[27] S. Passaggio,[27] F. C. Pastore,[27] C. Patrignani,[27] E. Robutti,[27] A. Santroni,[27] S. Tosi,[27] S. Bailey,[28] M. Morii,[28] M. L. Aspinwall,[29] W. Bhimji,[29] D. A. Bowerman,[29] P. D. Dauncey,[29] U. Egede,[29] I. Eschrich,[29] G. W. Morton,[29] J. A. Nash,[29] P. Sanders,[29] G. P. Taylor,[29] G. J. Grenier,[30] S.-J. Lee,[30] U. Mallik,[30] J. Cochran,[31] H. B. Crawley,[31] J. Lamsa,[31] W. T. Meyer,[31] S. Prell,[31] E. I. Rosenberg,[31] J. Yi,[31] M. Davier,[32] G. Grosdidier,[32] A. Höcker,[32] S. Laplace,[32] F. Le Diberder,[32] V. Lepeltier,[32] A. M. Lutz,[32] T. C. Petersen,[32] S. Plaszczynski,[32] M. H. Schune,[32] L. Tantot,[32] G. Wormser,[32] V. Brigljević,[33] C. H. Cheng,[33] D. J. Lange,[33] D. M. Wright,[33] A. J. Bevan,[34] J. P. Coleman,[34] J. R. Fry,[34] E. Gabathuler,[34] R. Gamet,[34] M. Kay,[34] R. J. Parry,[34] D. J. Payne,[34] R. J. Sloane,[34] C. Touramanis,[34] J. J. Back,[35] P. F. Harrison,[35] H. W. Shorthouse,[35] P. Strother,[35] P. B. Vidal,[35] C. L. Brown,[36] G. Cowan,[36] R. L. Flack,[36] H. U. Flaecher,[36] S. George,[36] M. G. Green,[36] A. Kurup,[36] C. E. Marker,[36] T. R. McMahon,[36] S. Ricciardi,[36] F. Salvatore,[36] G. Vaitsas,[36] M. A. Winter,[36] D. Brown,[37] C. L. Davis,[37] J. Allison,[38] R. J. Barlow,[38] A. C. Forti,[38] P. A. Hart,[38] F. Jackson,[38] G. D. Lafferty,[38] A. J. Lyon,[38] J. H. Weatherall,[38] J. C. Williams,[38] A. Farbin,[39] A. Jawahery,[39] D. Kovalskyi,[39] C. K. Lae,[39] V. Lillard,[39]

D. A. Roberts,[39] G. Blaylock,[40] C. Dallapiccola,[40] K. T. Flood,[40] S. S. Hertzbach,[40] R. Kofler,[40] V. B. Koptchev,[40] T. B. Moore,[40] S. Saremi,[40] H. Staengle,[40] S. Willocq,[40] R. Cowan,[41] G. Sciolla,[41] F. Taylor,[41] R. K. Yamamoto,[41] D. J. J. Mangeol,[42] M. Milek,[42] P. M. Patel,[42] A. Lazzaro,[43] F. Palombo,[43] J. M. Bauer,[44] L. Cremaldi,[44] V. Eschenburg,[44] R. Godang,[44] R. Kroeger,[44] J. Reidy,[44] D. A. Sanders,[44] D. J. Summers,[44] H. W. Zhao,[44] C. Hast,[45] P. Taras,[45] H. Nicholson,[46] C. Cartaro,[47] N. Cavallo,[47,†] G. De Nardo,[47] F. Fabozzi,[47,†] C. Gatto,[47] L. Lista,[47] P. Paolucci,[47] D. Piccolo,[47] C. Sciacca,[47] M. A. Baak,[48] G. Raven,[48] J. M. LoSecco,[49] T. A. Gabriel,[50] B. Brau,[51] T. Pulliam,[51] J. Brau,[52] R. Frey,[52] C. T. Potter,[52] N. B. Sinev,[52] D. Strom,[52] E. Torrence,[52] F. Colecchia,[53] A. Dorigo,[53] F. Galeazzi,[53] M. Margoni,[53] M. Morandin,[53] M. Posocco,[53] M. Rotondo,[53] F. Simonetto,[53] R. Stroili,[53] G. Tiozzo,[53] C. Voci,[53] M. Benayoun,[54] H. Briand,[54] J. Chauveau,[54] P. David,[54] Ch. de la Vaissière,[54] L. Del Buono,[54] O. Hamon,[54] M. J. J. John,[54] Ph. Leruste,[54] J. Ocariz,[54] M. Pivk,[54] L. Roos,[54] J. Stark,[54] S. T'Jampens,[54] P. F. Manfredi,[55] V. Re,[55] L. Gladney,[56] Q. H. Guo,[56] J. Panetta,[56] C. Angelini,[57] G. Batignani,[57] S. Bettarini,[57] M. Bondioli,[57] F. Bucci,[57] G. Calderini,[57] M. Carpinelli,[57] F. Forti,[57] M. A. Giorgi,[57] A. Lusiani,[57] G. Marchiori,[57] F. Martinez-Vidal,[57,‡] M. Morganti,[57] N. Neri,[57] E. Paoloni,[57] M. Rama,[57] G. Rizzo,[57] F. Sandrelli,[57] J. Walsh,[57] M. Haire,[58] D. Judd,[58] K. Paick,[58] D. E. Wagoner,[58] N. Danielson,[59] P. Elmer,[59] C. Lu,[59] V. Miftakov,[59] J. Olsen,[59] A. J. S. Smith,[59] E. W. Varnes,[59] F. Bellini,[60] G. Cavoto,[59,60] R. Faccini,[14,60] F. Ferrarotto,[60] F. Ferroni,[60] M. Gaspero,[60] M. A. Mazzoni,[60] S. Morganti,[60] M. Pierini,[60] G. Piredda,[60] F. Safai Tehrani,[60] C. Voena,[60] S. Christ,[61] G. Wagner,[61] R. Waldi,[61] T. Adye,[62] N. De Groot,[62] B. Franek,[62] N. I. Geddes,[62] G. P. Gopal,[62] E. O. Olaiya,[62] S. M. Xella,[62] R. Aleksan,[63] S. Emery,[63] A. Gaidot,[63] S. F. Ganzhur,[63] P.-F. Giraud,[63] G. Hamel de Monchenault,[63] W. Kozanecki,[63] M. Langer,[63] G. W. London,[63] B. Mayer,[63] G. Schott,[63] G. Vasseur,[63] Ch. Yeche,[63] M. Zito,[63] M. V. Purohit,[64] A. W. Weidemann,[64] F. X. Yumiceva,[64] D. Aston,[65] R. Bartoldus,[65] N. Berger,[65] A. M. Boyarski,[65] O. L. Buchmueller,[65] M. R. Convery,[65] D. P. Coupal,[65] D. Dong,[65] J. Dorfan,[65] D. Dujmic,[65] W. Dunwoodie,[65] R. C. Field,[65] T. Glanzman,[65] S. J. Gowdy,[65] E. Grauges-Pous,[65] T. Hadig,[65] V. Halyo,[65] T. Hryn'ova,[65] W. R. Innes,[65] C. P. Jessop,[65] M. H. Kelsey,[65] P. Kim,[65] M. L. Kocian,[65] U. Langenegger,[65] D. W. G. S. Leith,[65] S. Luitz,[65] V. Luth,[65] H. L. Lynch,[65] H. Marsiske,[65] S. Menke,[65] R. Messner,[65] D. R. Muller,[65] C. P. O'Grady,[65] V. E. Ozcan,[65] A. Perazzo,[65] M. Perl,[65] S. Petrak,[65] B. N. Ratcliff,[65] S. H. Robertson,[65] A. Roodman,[65] A. A. Salnikov,[65] R. H. Schindler,[65] J. Schwiening,[65] G. Simi,[65] A. Snyder,[65] A. Soha,[65] J. Stelzer,[65] D. Su,[65] M. K. Sullivan,[65] H. A. Tanaka,[65] J. Va'vra,[65] S. R. Wagner,[65] M. Weaver,[65] A. J. R. Weinstein,[65] W. J. Wisniewski,[65] D. H. Wright,[65] C. C. Young,[65] P. R. Burchat,[66] A. J. Edwards,[66] T. I. Meyer,[66] C. Roat,[66] S. Ahmed,[67] M. S. Alam,[67] J. A. Ernst,[67] M. Saleem,[67] F. R. Wappler,[67] W. Bugg,[68] M. Krishnamurthy,[68] S. M. Spanier,[68] R. Eckmann,[69] H. Kim,[69] J. L. Ritchie,[69] R. F. Schwitters,[69] J. M. Izen,[70] I. Kitayama,[70] X. C. Lou,[70] S. Ye,[70] F. Bianchi,[71] M. Bona,[71] F. Gallo,[71] D. Gamba,[71] C. Borean,[72] L. Bosisio,[72] G. Della Ricca,[72] S. Dittongo,[72] S. Grancagnolo,[72] L. Lanceri,[72] P. Poropat,[72,§] L. Vitale,[72] G. Vuagnin,[72] R. S. Panvini,[73] Sw. Banerjee,[74] C. M. Brown,[74] D. Fortin,[74] P. D. Jackson,[74] R. Kowalewski,[74] J. M. Roney,[74] H. R. Band,[75] S. Dasu,[75] M. Datta,[75] A. M. Eichenbaum,[75] H. Hu,[75] J. R. Johnson,[75] P. E. Kutter,[75] H. Li,[75] R. Liu,[75] F. Di Lodovico,[75] A. Mihalyi,[75] A. K. Mohapatra,[75] Y. Pan,[75] R. Prepost,[75] S. J. Sekula,[75] J. H. von Wimmersperg-Toeller,[75] J. Wu,[75] S. L. Wu,[75] Z. Yu,[75] and H. Neal[76]

(The *BABAR* Collaboration)

[1]*Laboratoire de Physique des Particules, F-74941 Annecy-le-Vieux, France*
[2]*Università di Bari, Dipartimento di Fisica and INFN, I-70126 Bari, Italy*
[3]*Institute of High Energy Physics, Beijing 100039, China*
[4]*University of Bergen, Inst. of Physics, N-5007 Bergen, Norway*
[5]*Lawrence Berkeley National Laboratory and University of California, Berkeley, CA 94720, USA*
[6]*University of Birmingham, Birmingham, B15 2TT, United Kingdom*
[7]*Ruhr Universität Bochum, Institut für Experimentalphysik 1, D-44780 Bochum, Germany*
[8]*University of Bristol, Bristol BS8 1TL, United Kingdom*
[9]*University of British Columbia, Vancouver, BC, Canada V6T 1Z1*
[10]*Brunel University, Uxbridge, Middlesex UB8 3PH, United Kingdom*
[11]*Budker Institute of Nuclear Physics, Novosibirsk 630090, Russia*
[12]*University of California at Irvine, Irvine, CA 92697, USA*
[13]*University of California at Los Angeles, Los Angeles, CA 90024, USA*
[14]*University of California at San Diego, La Jolla, CA 92093, USA*
[15]*University of California at Santa Barbara, Santa Barbara, CA 93106, USA*
[16]*University of California at Santa Cruz, Institute for Particle Physics, Santa Cruz, CA 95064, USA*
[17]*California Institute of Technology, Pasadena, CA 91125, USA*
[18]*University of Cincinnati, Cincinnati, OH 45221, USA*

[19]University of Colorado, Boulder, CO 80309, USA
[20]Colorado State University, Fort Collins, CO 80523, USA
[21]Technische Universität Dresden, Institut für Kern- und Teilchenphysik, D-01062 Dresden, Germany
[22]Ecole Polytechnique, LLR, F-91128 Palaiseau, France
[23]University of Edinburgh, Edinburgh EH9 3JZ, United Kingdom
[24]Università di Ferrara, Dipartimento di Fisica and INFN, I-44100 Ferrara, Italy
[25]Florida A&M University, Tallahassee, FL 32307, USA
[26]Laboratori Nazionali di Frascati dell'INFN, I-00044 Frascati, Italy
[27]Università di Genova, Dipartimento di Fisica and INFN, I-16146 Genova, Italy
[28]Harvard University, Cambridge, MA 02138, USA
[29]Imperial College London, London, SW7 2BW, United Kingdom
[30]University of Iowa, Iowa City, IA 52242, USA
[31]Iowa State University, Ames, IA 50011-3160, USA
[32]Laboratoire de l'Accélérateur Linéaire, F-91898 Orsay, France
[33]Lawrence Livermore National Laboratory, Livermore, CA 94550, USA
[34]University of Liverpool, Liverpool L69 3BX, United Kingdom
[35]Queen Mary, University of London, E1 4NS, United Kingdom
[36]University of London, Royal Holloway and Bedford New College, Egham, Surrey TW20 0EX, United Kingdom
[37]University of Louisville, Louisville, KY 40292, USA
[38]University of Manchester, Manchester M13 9PL, United Kingdom
[39]University of Maryland, College Park, MD 20742, USA
[40]University of Massachusetts, Amherst, MA 01003, USA
[41]Massachusetts Institute of Technology, Laboratory for Nuclear Science, Cambridge, MA 02139, USA
[42]McGill University, Montréal, QC, Canada H3A 2T8
[43]Università di Milano, Dipartimento di Fisica and INFN, I-20133 Milano, Italy
[44]University of Mississippi, University, MS 38677, USA
[45]Université de Montréal, Laboratoire René J. A. Lévesque, Montréal, QC, Canada H3C 3J7
[46]Mount Holyoke College, South Hadley, MA 01075, USA
[47]Università di Napoli Federico II, Dipartimento di Scienze Fisiche and INFN, I-80126, Napoli, Italy
[48]NIKHEF, National Institute for Nuclear Physics and High Energy Physics, NL-1009 DB Amsterdam, The Netherlands
[49]University of Notre Dame, Notre Dame, IN 46556, USA
[50]Oak Ridge National Laboratory, Oak Ridge, TN 37831, USA
[51]Ohio State University, Columbus, OH 43210, USA
[52]University of Oregon, Eugene, OR 97403, USA
[53]Università di Padova, Dipartimento di Fisica and INFN, I-35131 Padova, Italy
[54]Universités Paris VI et VII, Lab de Physique Nucléaire H. E., F-75252 Paris, France
[55]Università di Pavia, Dipartimento di Elettronica and INFN, I-27100 Pavia, Italy
[56]University of Pennsylvania, Philadelphia, PA 19104, USA
[57]Università di Pisa, Dipartimento di Fisica, Scuola Normale Superiore and INFN, I-56127 Pisa, Italy
[58]Prairie View A&M University, Prairie View, TX 77446, USA
[59]Princeton University, Princeton, NJ 08544, USA
[60]Università di Roma La Sapienza, Dipartimento di Fisica and INFN, I-00185 Roma, Italy
[61]Universität Rostock, D-18051 Rostock, Germany
[62]Rutherford Appleton Laboratory, Chilton, Didcot, Oxon, OX11 0QX, United Kingdom
[63]DSM/Dapnia, CEA/Saclay, F-91191 Gif-sur-Yvette, France
[64]University of South Carolina, Columbia, SC 29208, USA
[65]Stanford Linear Accelerator Center, Stanford, CA 94309, USA
[66]Stanford University, Stanford, CA 94305-4060, USA
[67]State Univ. of New York, Albany, NY 12222, USA
[68]University of Tennessee, Knoxville, TN 37996, USA
[69]University of Texas at Austin, Austin, TX 78712, USA
[70]University of Texas at Dallas, Richardson, TX 75083, USA
[71]Università di Torino, Dipartimento di Fisica Sperimentale and INFN, I-10125 Torino, Italy
[72]Università di Trieste, Dipartimento di Fisica and INFN, I-34127 Trieste, Italy
[73]Vanderbilt University, Nashville, TN 37235, USA
[74]University of Victoria, Victoria, BC, Canada V8W 3P6
[75]University of Wisconsin, Madison, WI 53706, USA
[76]Yale University, New Haven, CT 06511, USA

(Dated: June 2, 2003)

We present results of searches for exclusive charged-B-meson decays to $K^{\pm}\pi^{\mp}\pi^{\pm}$ from approximately 61.6 million $B\overline{B}$ pairs collected at the *BABAR* detector. We measure the following branching fractions averaged over charged-conjugate states: $\mathcal{B}(B^{+} \rightarrow K^{*0}(892)\pi^{+}, K^{*0} \rightarrow K^{+}\pi^{-}) = (10.3 \pm 1.2^{+1.0}_{-2.7}) \times 10^{-6}$, $\mathcal{B}(B^{+} \rightarrow f_0(980)K^{+}, f_0 \rightarrow \pi^{+}\pi^{-}) = (9.2 \pm 1.2^{+2.1}_{-2.6}) \times 10^{-6}$

and $\mathcal{B}(B^+ \to \overline{D}^0\pi^+, \overline{D}^0 \to K^+\pi^-) = (184.6 \pm 3.2 \pm 9.7) \times 10^{-6}$, and give 90% confidence-level upper limits on the branching fractions of the following channels: $\mathcal{B}(B^+ \to \rho^0(770)K^+) < 6.2 \times 10^{-6}$ and $\mathcal{B}(B^+ \to K^+\pi^-\pi^+$ non-resonant$) < 17 \times 10^{-6}$.

PACS numbers: 13.25.Hw, 12.15.Hh, 11.30.Er

The study of charmless hadronic B decays can make important contributions to the understanding of CP violation in the Standard Model as well as to models of hadronic decays. The measurement of B^+-meson [1] decays to the final state $K^+\pi^-\pi^+$ via intermediate resonances can be used to search for weak phases and direct CP violation.

The data used in this analysis were collected at the PEP-II asymmetric e^+e^- storage ring with the *BABAR* detector, described in detail elsewhere [2]. The data sample consists of 61.6 million $B\overline{B}$ pairs, corresponding to an integrated luminosity of 56.4 fb^{-1}, collected at the $\Upsilon(4S)$ resonance. We assume that the $\Upsilon(4S)$ decays equally to neutral and charged B meson pairs.

The $K^+\pi^-\pi^+$ final state can be represented in a Dalitz plot [3], in which the many resonant B decay modes form overlapping bands. Their interference means that the whole Dalitz plot should be considered before assigning a branching fraction to a specific mode. This analysis divides the Dalitz plot into eight regions, each of which is expected to be dominated by a particular contribution. First the yields in these regions are determined, using a maximum-likelihood fit. We then interpret the yields as branching fractions, assuming a specific model for the contributions to the Dalitz plot. We also consider the uncertainty of the model and the effect of interference between these contributions. The analysis methods are described in further detail in [4].

The definitions of the regions are given in Table I. Region I is expected to be dominated by the $K^{*0}(892)$. The primary resonance contribution to Region II, labeled "higher K^{*0}", is not currently known. The areas where these bands cross the $\pi\pi$ resonances are excluded to limit biases from interference. Region III is dominated by the production of $\overline{D}^0\pi^+$. The relatively high branching fraction for this mode allows it to be used to correct for differences between data and simulated events and to evaluate systematic uncertainties. Regions IV and V are expected to be dominated by the $\rho(770)$ and $f_0(980)$, respectively. The resonance contributions to Region VI ("higher f") are not well defined. The area where these regions intersect the $\overline{D}^0$ band is excluded. Region VII, denoted "high mass", could contain higher charmless and charmonium resonances as well as a non-resonant contribution. Region VIII is dominated by $\chi_{c0}K^+$.

Hadronic events are selected based on track multiplicity and event topology. Backgrounds from non-hadronic events are reduced by requiring the ratio of Fox-Wolfram moments H_2/H_0 [5] to be less than 0.98. Candidate B decays are formed by combining three charged tracks, where each track is required to have at least 12 hits in the drift chamber, a minimum transverse momentum of 100 MeV/c, and is consistent with originating from the beam-spot.

TABLE I: Regions of the $K^+\pi^-\pi^+$ Dalitz plot and signal yields obtained. The symbol "!" is used to imply exclusion.

Region	Selection Criteria (GeV/c^2)		Signal Yield
I	$0.816 < m_{K\pi} < 0.976$	$m_{\pi\pi} > 1.5$ $!(3.355 < m_{\pi\pi} < 3.475)$	$161 \pm 18 \pm 4$
II	$0.976 < m_{K\pi} < 1.8$	$m_{\pi\pi} > 1.5$ $!(3.355 < m_{\pi\pi} < 3.475)$	$405 \pm 28^{+12}_{-13}$
III	$1.835 < m_{K\pi} < 1.895$	$!(3.355 < m_{\pi\pi} < 3.475)$	$3755 \pm 66 \pm 11$
IV	$!(1.8 < m_{K\pi} < 1.9)$	$0.6 < m_{\pi\pi} < 0.9$	$66 \pm 15^{+3}_{-7}$
V	$!(1.8 < m_{K\pi} < 1.9)$	$0.9 < m_{\pi\pi} < 1.1$	$179 \pm 19 \pm 5$
VI	$!(1.8 < m_{K\pi} < 1.9)$	$1.1 < m_{\pi\pi} < 1.5$	$126 \pm 19 \pm 5$
VII	$m_{K\pi} > 1.9$	$m_{\pi\pi} > 1.5$ $!(3.355 < m_{\pi\pi} < 3.475)$	$133 \pm 23^{+9}_{-22}$
VIII	$m_{K\pi} > 1.9$	$3.37 < m_{\pi\pi} < 3.46$	$26 \pm 6 \pm 1$

Charged pions and kaons are identified using energy loss ($\mathrm{d}E/\mathrm{d}x$) in the tracking system, and, for tracks with momenta above 700 MeV/c, the Cherenkov angle and number of photons measured by the Cherenkov detector. Kaons are selected by applying selection criteria to the product of the likelihood ratios determined from these measurements. The efficiency of selecting kaons is approximately 80%, while the probability of misidentifying pions as kaons is below 5%, up to a laboratory momentum of 4.0 GeV/c. Pions are required to fail both the kaon selection and an electron selection based on information from $\mathrm{d}E/\mathrm{d}x$ and the calorimeter. The efficiency for selecting pions is approximately 98%.

Signal decays are identified using two kinematic variables: ΔE, the difference between the center-of-mass (CM) energy of the B candidate and $\sqrt{s}/2$, where $\sqrt{s}$ is the total CM energy, and the beam-energy-substituted mass $m_{\mathrm{ES}} = \sqrt{(s/2 + \mathbf{p}_i \cdot \mathbf{p}_B)^2/E_i^2 - \mathbf{p}_B^2}$, where the B momentum $\mathbf{p}_B$ and the four-momentum of the initial state $(E_i, \mathbf{p}_i)$ are defined in the laboratory frame. The ΔE and m_{ES} distributions of signal events are Gaussian with resolutions of 20 MeV and 2.7 MeV/c^2, respectively.

The dominant source of background is from light quark and charm continuum production. To suppress this, two event-shape variables are computed in the CM frame. The first is the cosine of the angle θ_T between the thrust axis of the selected B candidate and the thrust axis of the rest of the event. For continuum backgrounds, the distribution of $|\cos\theta_T|$ is strongly peaked towards unity because the daughters of the reconstructed candidate tend to lie along the primary jet axis. The low CM momentum of the B mesons in the $\Upsilon(4S)$ decay means that the distribution is essentially uniform for signal events. A requirement of $|\cos\theta_T| < 0.9$ is applied to all regions except Region III ($\overline{D}^0$). This selection removes about 60% of the continuum background while retaining over 90% of the signal. The second event-shape variable is a Fisher discriminant [6] ($\mathcal{F}$). This is a linear combination of the angles between the B candidate momentum and the beam axis, and between the B candidate thrust axis and the beam axis, and the energy flow of the rest of the event into each of 9 independent concentric 10° cones around the thrust axis of the reconstructed B [7].

There are also B decay backgrounds mainly from three sources: $B \to D$ decays, charmless four-body decays, and three-body decays with one or more particles misidentified. These backgrounds are reduced by the particle identification selections and, where possible (J/ψ X, $\psi(2S)$ X), removed by vetoing regions of the invariant-mass spectra. Where this is not possible a component is included in the likelihood fit, or if the contribution is small it is instead subtracted from the signal yield.

We form Probability Density Functions (PDFs) with parameters $\vec{\alpha}$ for the 3 variables ($\vec{x}$) $m_{\rm ES}$, ΔE and $\mathcal{F}$ in each region. We find the correlations among these variables to be small; as such, for each hypothesis l (signal, continuum background, and B background), we can form a product P_l, which models that hypothesis. The likelihood for an event j is the sum of the products over the M hypotheses, with each product weighted by the number of events in that hypothesis n_l. A product over the N events in the data sample of the per-event likelihoods along with a Poisson factor forms the total likelihood function $\mathcal{L}$, written in Eq. (1).

$$\mathcal{L} = \exp\left(-\sum_{i=1}^{M} n_i\right) \prod_{j=1}^{N} \left(\sum_{l=1}^{M} n_l\, P_l(\vec{\alpha}, \vec{x_j})\right). \qquad (1)$$

The parameters of the signal and B background PDFs are determined from Monte Carlo (MC) simulations, whilst those of the continuum background are taken from ($m_{\rm ES}$, ΔE) sideband data. The $m_{\rm ES}$ PDFs are a gaussian for signal, and an Argus threshold function [8] for continuum background. The ΔE PDFs are two Gaussians with equal means for the signal and a first-degree polynomial for the background. The $\mathcal{F}$ PDFs are, for both signal and background, Gaussians with different widths above and below the mean.

The signal yields for the regions of the $K^+\pi^-\pi^+$ Dalitz plot are shown in Table I. The systematic uncertainty is from the uncertainties on the PDF parameters and from B background subtraction. The yields are found to be statistically significant in all regions ($> 5\sigma$), where the statistical significance is taken (in units of the standard deviation (σ)) as $\sqrt{-2\log(\mathcal{L}_{max}/\mathcal{L}_{(n_{sig}=0)})}$.

Figure 1 shows the Dalitz plot for data events within the signal region $5.2715 < m_{ES} < 5.2865\,\mathrm{GeV}/c^2$ that have a per-event signal to background likelihood ratio, formed from the ΔE and $\mathcal{F}$ PDFs, greater than 5. The $\overline{D}^0\ \pi^+$ signal is clear as a narrow band in the $m_{K\pi}$ spectrum. To illustrate the expected background distribution, events passing the same likelihood selection but having a value of m_{ES} between $5.25 < m_{ES} < 5.26\,\mathrm{GeV}/c^2$ are shown alongside. The size of this sideband is chosen to contain approximately the expected number of background events.

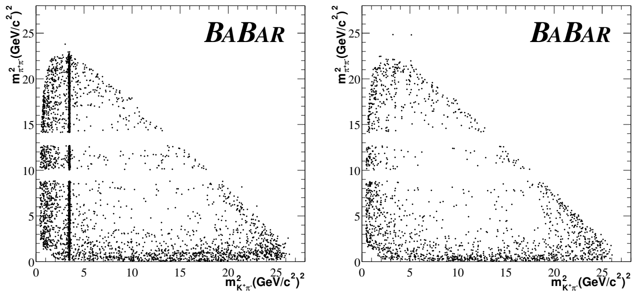

FIG. 1: Dalitz plots showing the observed distribution in the signal $m_{\rm ES}$ region (left) and continuum background from the $m_{\rm ES}$ sideband (right)

Figure 2 shows background-subtracted, efficiency-corrected plots of the resonant mass and helicity angle distributions for Regions I and V. The plots have been overlaid with the distribution of the expected dominant resonance using Breit–Wigner line-shapes for the mass distributions, $\cos^2\theta_H$ for the $K^{*0}(892)$ angular distribution and a first-degree polynomial for the scalar $f_0(980)$ angular distribution allowing for interference with the vector $\rho(770)$. There is good agreement between the overlaid and observed distributions indicating that the expected resonances are indeed dominant in these regions. Figure 2 also shows plots for Region II produced in the same way. It is not clear from these distributions which resonances are present but we can conclude that they cannot be explained by a single resonance. A similar distribution has been observed on the LASS experiment [9].

Regions III and VIII have negligible contributions from $B^+ \to K^+\pi^-\pi^+$ channels other than $\overline{D}^0\pi^+$ and $\chi_{c0}K^+$, respectively. $\overline{D}^0\pi^+$ and $\chi_{c0}K^+$ do not contribute to other regions. The branching fractions for these channels are defined by $\mathcal{B} = \mathrm{Y}/\mathrm{N}_{B\overline{B}}\,\varepsilon$, where Y is the signal yield and $\mathrm{N}_{B\overline{B}} = (61.6 \pm 0.7) \times 10^6$ is the number of $B\overline{B}$ events in the sample. The reconstruction efficiency, ε, is calculated using a signal MC sample and is corrected for MC/data discrepancies in tracking and particle identification.

For the other regions, we calculate the branching fractions from the measured yields taking into account the resonance cross-feed and model dependence. Y becomes a vector of the yields in each Dalitz region, $\mathcal{B}$ becomes a vector of the branching fractions and the efficiency be-

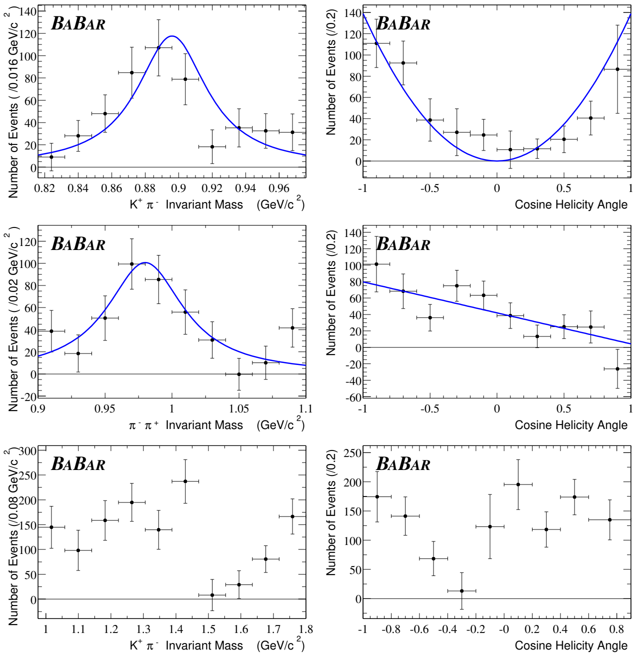

FIG. 2: Projection plots of the resonant mass and cosine of the helicity angle for Regions I, V and II.

comes a matrix M the elements of which are the probability of an event of a particular decay to be found in a particular region, hence: $\mathcal{B} = \mathrm{M}^{-1}\ \mathrm{Y}/\mathrm{N}_{B\overline{B}}$. The elements of M are estimated using signal MC, correcting for MC/data differences in tracking, particle identification and differences between signal MC and our resonance model.

In our resonance model we assume one dominant contribution per region. The decay modes in the chosen model are given in Table II, along with the alternatives considered as systematic uncertainties. The masses and widths are taken from the Review of Particle Physics [10], and non-relativistic Breit–Wigner line-shapes are used for all channels except for the broad $\rho(770)$ resonance, where we use a relativistic Breit–Wigner lineshape with Blatt–Weisskopf damping [11]. Model uncertainties on the branching fractions are evaluated that take into consideration alternative resonances and lineshapes, uncertainties on resonance parameters, as well as the possibility that the yield measured in Region VII is not due to a non-resonant component and so does not extend into the other regions. The model uncertainty is the quadratic sum of all the variations in the branching fraction due to these individual changes. There are uncertainties due to the interference between the resonances that are also evaluated.

Table III gives the branching fractions obtained from the vector of yields with statistical, reconstruction-systematic, resonance-model and interference uncertainties. For most channels, the largest contribution to the reconstruction-systematic uncertainty is from the uncer-

TABLE II: A summary of the model used to calculate branching fractions.

Decay Mode	Lineshape	Mass (MeV/c^2)	Width (MeV/c^2)	Alternative Resonance
$K^{*0}(892)\pi^+$	BW	896.10 ± 0.27	50.7 ± 0.6	-
$K_0^{*0}(1430)\pi^+$	BW (LASS[9])	1412 ± 6	294 ± 23	$K_2^{*0}(1430)$,$K_1^{*0}(1680)$
$\rho^0(770)K^+$	Blatt-W[11]	769.0 ± 0.9	150.9 ± 1.7	-
$f_0(980)K^+$	BW (Flatté[12])	980 ± 10	70 ± 30	-
$f_2(1270)K^+$	BW	1275 ± 12	185 ± 30	$f_0(1370)$, $f_2(1430)$
non-resonant	flat	all masses	-	-

TABLE III: The branching fractions and uncertainties for the channels measured.

Channel	BF	uncertainties ($\times 10^{-6}$)			
	($\times 10^{-6}$)	stat	sys	model	interference
$K^{*0}(892)\pi^+, K^{*0} \to K^+\pi^-$	10.3	± 1.2	± 0.7	$^{+0.4}_{-2.5}$	± 0.6
"higher K^{*0}"$\pi^+, K^{*0} \to K^+\pi^-$	25.1	± 2.0	± 2.9	$^{+9.4}_{-0.5}$	± 4.9
$\overline{D}^0\ \pi^+, \overline{D}^0 \to K^+\pi^-$	184.6	± 3.2	± 9.7	-	-
$\rho^0(770)K^+, \rho^0(770) \to \pi^+\pi^-$	3.9	± 1.2	$^{+0.3}_{-0.6}$	$^{+0.3}_{-3.2}$	± 1.2
$f_0(980)K^+, f_0 \to \pi^+\pi^-$	9.2	± 1.2	± 0.6	$^{+1.2}_{-1.9}$	± 1.6
"higher f"$K^+, f \to \pi^+\pi^-$	3.2	± 1.2	± 0.5	$^{+5.8}_{-2.4}$	± 1.5
Non-resonant	5.2	± 1.9	$^{+0.8}_{-1.8}$	$^{+3.3}_{-7.5}$	± 6.4
$\chi_{c0}K^+, \chi_{c0} \to \pi^+\pi^-$	1.5	± 0.4	± 0.1	-	-

tainties on the PDF parameters, the B background uncertainty is dominant for $B^+ \to \rho^0(770)K^+$ and non-resonant.

In conclusion, we have made measurements of the branching fractions for the following channels with a statistical significance greater than 5σ. $\mathcal{B}(B^+ \to K^{*0}(892)\pi^+, K^{*0} \to K^+\pi^-) = (10.3 \pm 1.2^{+1.0}_{-2.7}) \times 10^{-6}$, $\mathcal{B}(B^+ \to f_0(980)K^+, f_0 \to \pi^+\pi^-) = (9.2 \pm 1.2^{+2.1}_{-2.6}) \times 10^{-6}$, $\mathcal{B}(B^+ \to \chi_{c0}K^+, \chi_{c0} \to \pi^+\pi^-) = (1.46 \pm 0.35 \pm 0.12) \times 10^{-6}$, $\mathcal{B}(B^+ \to \overline{D}^0\pi^+, \overline{D}^0 \to K^+\pi^-) = (184.6 \pm 3.2 \pm 9.7) \times 10^{-6}$ $\mathcal{B}(B^+ \to$"higher K^{*0}"$\pi^+) = (25.1 \pm 2.0^{+11.0}_{-5.7}) \times 10^{-6}$, where "higher K^{*0}" means any combination of $K_0^{*0}(1430), K_2^{*0}(1430)$ and $K_1^{*0}(1680)$. The first uncertainty is statistical and the second is systematic. This analysis has taken into account the uncertainty in the knowledge of the nature and parameterization of these resonances as well as interference between them, and these uncertainties are included (added in quadrature) in the above systematic value. Using the value of $\mathcal{B}(K^{*0}(892) \to K^+\pi^-) = 2/3$, we find $\mathcal{B}(B^+ \to K^{*0}(892)\pi^+) = (15.5 \pm 1.8^{+1.5}_{-3.2}) \times 10^{-6}$, which is consistent with, and more precise than, previous measurements [13].

We give 90% confidence-level upper limits for the branching fractions of the following channels, including the non-resonant component. $\mathcal{B}(B^+ \to \rho^0(770)K^+) < 6.2 \times 10^{-6}$, $\mathcal{B}(B^+ \to K^+\pi^-\pi^+$ non-resonant$) < 17 \times 10^{-6}$, $\mathcal{B}(B^+ \to$"higher f"$K^+) < 12 \times 10^{-6}$, where "higher f" means any combination of $f_2(1270)$, $f_0(1370)$ and $f_2(1430)$.

We are grateful for the excellent luminosity and machine conditions provided by our PEP-II colleagues, and for the substantial dedicated effort from the computing organizations that support *BABAR*. The collaborating institutions wish to thank SLAC for its support and kind hospitality. This work is supported by DOE and

NSF (USA), NSERC (Canada), IHEP (China), CEA and CNRS-IN2P3 (France), BMBF and DFG (Germany), INFN (Italy), FOM (The Netherlands), NFR (Norway), MIST (Russia), and PPARC (United Kingdom). Individuals have received support from the A. P. Sloan Foundation, Research Corporation, and Alexander von Humboldt Foundation.

---

* Also with Università di Perugia, Perugia, Italy
† Also with Università della Basilicata, Potenza, Italy
‡ Also with IFIC, Instituto de Física Corpuscular, CSIC-Universidad de Valencia, Valencia, Spain
§ Deceased

[1] Charge-conjugate states are included throughout this document.
[2] *BABAR* Collaboration, B. Aubert *et al.*, Nucl. Instr. Meth. A **479** 1 (2002).
[3] R. H. Dalitz, Phil. Mag. **44** 1068 (1953).
[4] *BABAR* Collaboration, B. Aubert *et al.*, hep-ex/0303022 (SLAC-PUB-9676).
[5] G. C. Fox and S. Wolfram, Phys. Rev. Lett. **41** 1581 (1978).
[6] R. A. Fisher, Ann. Eugenics **7** 179 (1936); G. Cowan *Statistical Data Analysis*, 51 (Oxford University Press, 1998).
[7] CLEO Collaboration, D. M. Asner *et al.*, Phys. Rev. D **53** 1039 (1996).
[8] ARGUS Collaboration, H. Albrecht *et al.*, Z. Phys. C **48** 543 (1990).
[9] D. Aston *et al.*, Nucl. Phys. B **296** 493 (1988).
[10] Particle Data Group, Phys. Rev. D **66** 010001 (2002).
[11] J. M. Blatt and V. F. Weisskopf, *Theoretical Nuclear Physics* 361 (Wiley, New York, 1952).
[12] S. M. Flatté, Phys. Lett. B **63** 224 (1976).
[13] Belle Collaboration, K. Abe *et al.*, Phys. Rev. D **65** 092005 (2002).